doi: 10.56761/EFRE2022.S5-P-000702

Influence of a voltage pulse rise time and pressure of air and nitrogen on the parameters of runaway electron beams

D.V. Beloplotov[1], V.F. Tarasenko[1,2], D.A. Sorokin[1,]*

[1]*Institute of High Current Electronics SB RAS, Tomsk, Russia*
[2]*National Research Tomsk Polytechnic University, Tomsk, Russia*
[*]*SDmA-70@loi.hcei.tsc.ru*

Abstract. The generation of runaway electron beams with different high-voltage generators has been studied. The current of runaway electron beams generated during breakdown in air and nitrogen at a pressure range of 25–100 kPa was measured. It has been shown the conditions for electron runaway are easily realized at voltage pulse rise time of up to 200 ns. It has been found that to measure electron beam current at minimum voltages (tens of kilovolts) and a long rise time of the voltage pulse, anodes from a grid with a small cell size should be used. It follows from this work and the results of our previous studies that the generation of a runaway electron initiates the formation of a streamer, the development of which leads to an initial drop in the voltage across the gap.
Keywords: runaway electron beams, air, nitrogen, atmospheric pressure, voltage pulse front.

1. Introduction

The generation of runaway electrons (REs) is a fundamental physical phenomenon that takes place in natural discharges, in laboratory discharges, including spark discharges with one-meter gaps, as well as in installations for studying a controlled thermonuclear reaction. The possibility of the appearance of runaway electrons was predicted at the beginning of the last century in relation to atmospheric discharges in the upper atmosphere [1]. REs are generated in various gases when a strong electric field is applied to the gap. If the electron between collisions with gas particles gains more energy than it loses in inelastic collisions, then it goes into the runaway mode. In this case, the energy of the electron will increase and can reach high values. This phenomenon is due to the fact that the cross section for inelastic energy losses in collisions has a maximum at a certain electron energy (~100 eV for nitrogen) and then decreases with an increase in energy up to ~1 MeV. To implement the electron runaway mode, it is more advantageous to use cathodes with a small radius of curvature, which facilitates the initial acceleration of electrons. To date, a great deal of experience has been accumulated in the experimental production of REs in laboratory discharges in centimeter gaps and in modeling the conditions for their generation [2–8]. However, most studies were carried out with one pulse generator, the voltage pulse rise time of which did not change.

This paper presents the results of systematic studies on the influence of the voltage pulse rise time on the generation of runaway electron beams during breakdown in air and nitrogen at a pressure range of 25–100 kPa. In the experiments, we used three generators with different durations of the voltage pulse front and a tip-to-plane gap. This work continues our research on the generation of runaway electrons [2, 7–10].

2. Experimental setup and measuring equipment

The experiments were performed on the setup with three generators and discharge chamber with variable air and nitrogen pressures. A GIN-35NP generator (#1), which was fabricated in the laboratory, has a maximum voltage amplitude of up to 35 kV, a pulse FWHM of $\tau_{0.5} \approx 270$ ns, and a rise time of $\tau_{0.1–0.9} \approx 200$ ns. An NPG-18/3500N generator (#2) generates voltage pulses with an amplitude of up to 36 kV (mismatched load) at $\tau_{0.5} \approx 7$ ns and $\tau_{0.1–0.9} \approx 4$ ns. A GIN-100-01 generator (#3) generates voltage pulses with an amplitude of up to 62 kV (mismatched load) at $\tau_{0.5} \approx 5$ ns and $\tau_{0.1–0.9} \approx 0.7$ ns. The block diagram of experimental setup is shown in Fig.1.

High-voltage electrode (*4*) with a length of 5 mm was made of a part of a sewing needle. The base diameter was 1 mm, and the radius of curvature at the end was 75 μm. The needle was fixed on

a cone that was gradually transformed into a cylinder with a diameter of 6 mm. The gap length was 8.5 mm.

The voltage pulses were measured with a capacitive voltage divider. Voltage across the gap when applying generators no. 2 and 3 was reconstructed from the incident and reflected waves. Electric signals from the probes were recorded with a KeySight MSOS804A (6 GHz, 20 GSa/s) or a LeCroy WaveMaster 830Zi-A digital oscilloscopes (30 GHz, 80 GSa/s). The experiments were carried out in the single-pulse mode.

The previously obtained results with these generators and discharge chamber on the discharge formation with taking into account the dynamic displacement current induced by a streamer are presented in [8–10]. The plasma emission evolution at the breakdown stage was studied with high-speed image capture methods. For this, a Hamamatsu C10910-05 ultra-high-speed streak camera and a HSFC-PRO four-channel ICCD camera were used.

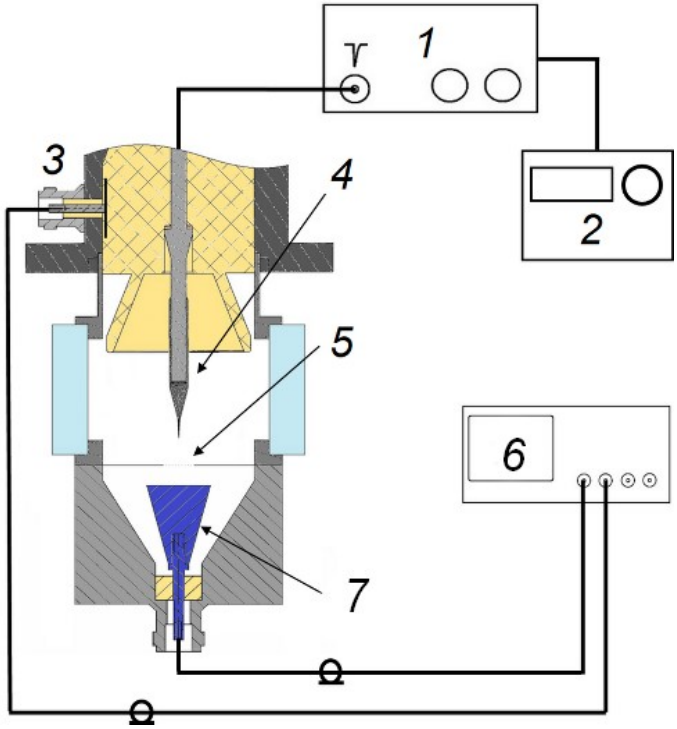

Fig.1. Block diagram of experimental setup: *1* – high-voltage generator, *2* – trigger generator, *3* – capacitive voltage divider, *4* – needle electrode, *5* – plane electrode from grid or foil, *6* – oscilloscope, *7* – collector.

3. Results

Voltage and supershort avalanche electron beam (SAEB) measurements were performed for all three generators. With generator #1, the open circuit voltage was chosen to be 34 kV. Under these conditions, at an air pressure of 25 kPa, the breakdown of the gap was recorded with different probabilities at voltages of 15–26 kV. With increasing pressure, the amplitude of the voltage pulses during the breakdown of the gap increased and reached 30 kV at a pressure of 100 kPa. At the same time, the SAEB amplitude decreased. Fig.2 shows the waveforms of voltage as well as SAEB current pulses in air at a pressure of 25 kPa.

The SAEB current waveforms in Figs.2–4 and subsequent ones correspond to waveforms of voltage pulses of the same color. In these experiments, a grid with a transparency of 62% served as the anode. The grid had a mesh size of 400 μm × 400 μm. More than 30 pulses were recorded, in Fig.2 shows some of them with different breakdown voltages. At the minimum breakdown voltage

(≈15 kV, waveform *2*), the SAEB was very small. However, under breakdown conditions at a voltage of ≈20 kV (waveforms 3) and above, SAEB current was stably measured with the collector with a diameter of receiving part of 20 mm. To estimate the electron energy, the grounded plane electrode was made a 2 μm kimfoil ($C_{16}H_{14}O_3$) film coated with a 0.2 μm thickness aluminum layer were placed. This film traps electrons with energies less than 10 keV. At a pressure of 25 kPa, SAEB with approximately the same amplitude at a breakdown voltage of 25 kV was recorded both behind the grid with a transparency of 62% and behind the kimfoil film.

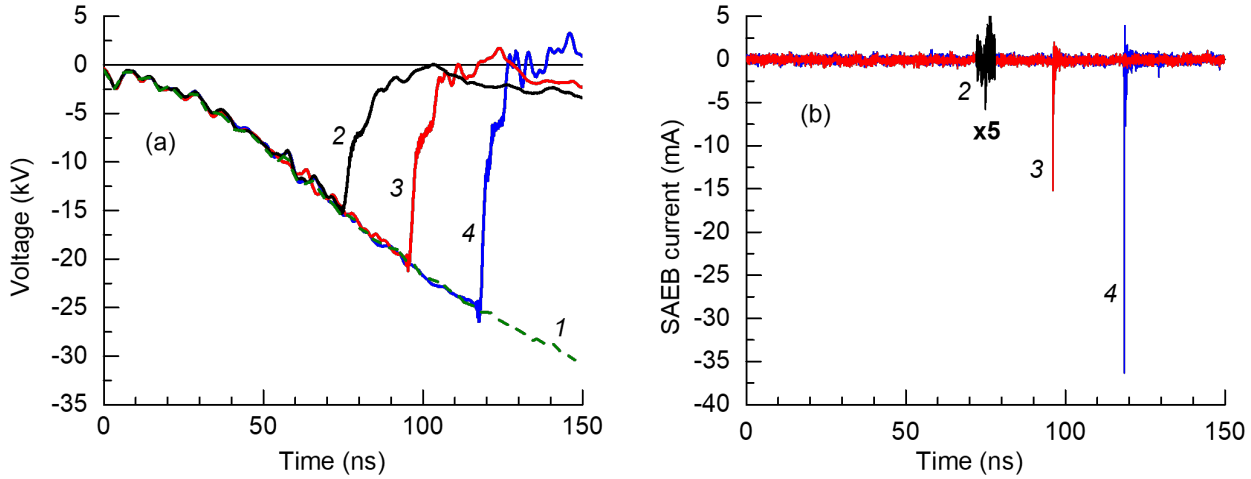

Fig.2. Waveforms of (a) voltage and (b) SAEB current pulses measured behind the anode made of a grid. The collector 20 mm in diameter was used. Air at a pressure of 25 kPa. *1* – no-load mode; *2–4* – different discharge implementations. Generator #1.

In the follow part of voltage waveforms, a step with a voltage of ≈7 kV is visible. It is caused by the formation of a quasi-stationary diffuse discharge. The SAEB current amplitude increased with increasing voltage across the gap, Fig.2b. Waveforms *4* were obtained at the maximum breakdown voltage under these conditions. The voltage of the generator #1 was chosen so that breakdown occurred at the leading edge of the voltage pulse. Due to the relatively low rate of rise of voltage across the gap (*dU*/*dt*), the spread of breakdown voltages was large. However, for each pulse with a breakdown voltage of ≥20 kV at a pressure 25 kPa air, SAEB pulses were recorded. At an air pressure of 100 kPa, the electron beam began to be recorded at a voltage of ≥26 kV and only with the grid anode.

Reducing the leading edge of the voltage pulse increases the electric field strength during SAEB generation. In particular, SAEB current pulses was recorded during the voltage pulse decay, Fig.3. The amplitude of the SAEB current pulses under these conditions increased and SAEB was further weakened by installing a second mesh in front of the collector, as well as decreasing the diameter of the receiving part of the collector. Under these conditions, SAEB generation was observed at the maximum voltage across the gap and at the decay of the voltage pulse. The beam current, as in [9, 10], initiated the development of a streamer, the movement of the front of which to the anode led to the beginning of a voltage drop across the gap. Under these conditions, steps are visible on the waveforms of voltages *2*, *3*, *4*, and *5*, which appears when the streamer front arrives at the anode. In Fig.2a, such a step is noticeable due to the slower voltage growth rate across the gap.

With a decrease the rise time of voltage pulse up to 0.7 ns, the minimum breakdown voltage of the gap filled with atmospheric pressure air increased up to ≥50 kV. Fig.4 shows the waveforms of voltage as well as SAEB current pulses for these conditions.

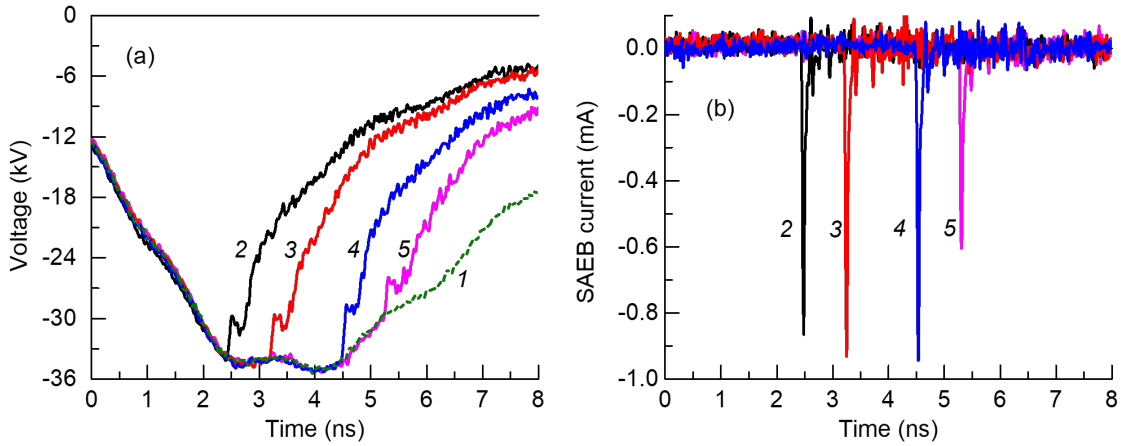

Fig.3. Waveforms of (a) voltage and (b) SAEB current pulses measured behind the anode made of a grid. The collector 3 mm in diameter was used. It was shielded with an additional grounded grid. Air at a pressure of 50 kPa. *1* – no-load mode; *2–5* – different discharge implementations. Generator #2.

Since the amplitude of SAEB current pulses increased with increasing voltage, the SAEB was further weakened by reducing the diameter of the receiving part of the collector. Under these conditions, SAEB generation was observed at the maximum voltage across the gap and at its front. Fig.4 shows waveforms obtained when filling the gap with nitrogen. With the generator # 3, electron beam was recorded behind not only the mesh and film made of kimfol, but also behind the aluminum foil 10 μm thick. Hence, it follows that the energy of some of the electrons in SAEB exceeded 40 keV.

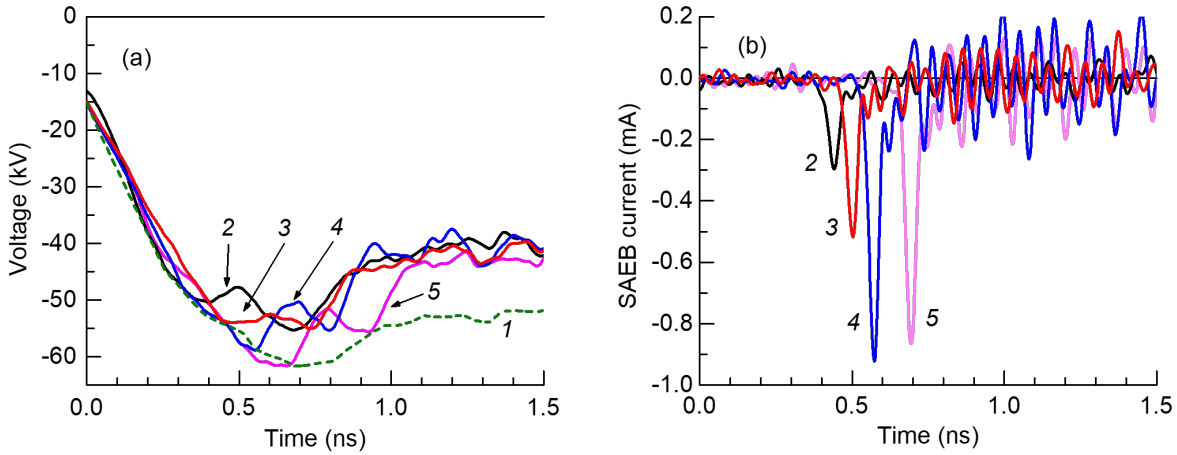

Fig.4. Waveforms of (a) voltage and (b) SAEB current pulses measured behind the anode made of a grid. The collector 3 mm in diameter was used. It was shielded with an additional grounded grid. Nitrogen at a pressure of 100 kPa. *1* – no-load mode; *2–5* – different discharge implementations. Generator #3.

Replacing air with nitrogen did not significantly affect the SAEB parameters, as well as its dependence on the rise time and voltage pulse amplitude. With a short leading edge of the voltage pulse, the voltage value during the step on waveforms *2*, *3*, *4*, and *5*, which is associated with the arrival of the streamer at the anode, increased in comparison with those obtained in Fig.3.

4. Discussion

The studies carried out confirm that the generation of fast and runaway electrons in an inhomogeneous electric field is a common physical phenomenon. We call fast electrons, which gain

energy from fractions of hundreds of eV to units of keV, but then lose it in collisions with gas particles and do not leave the gap. We call runaway electrons that gain energy in tens of kiloelectronvolts or more. REs have a higher energy and are recorded by a collector behind a mesh or thin foil anode. The first electrons appear near the tip due to field emission due to the high strength of the electric field. Fig.5 shows the results of calculating the electric field strength and the potential distribution in the discharge gap in the absence of plasma.

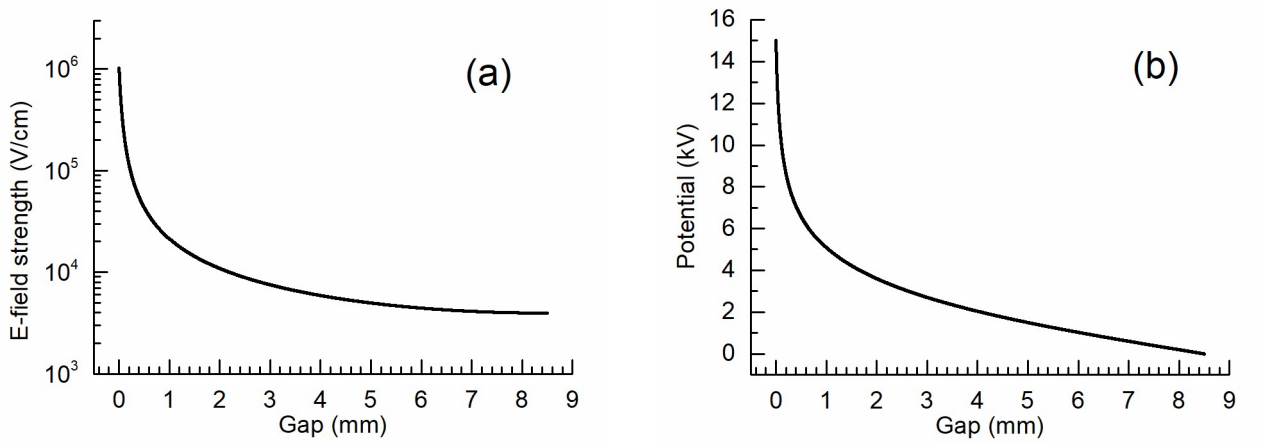

Fig.5. Distribution of electric field strength (a) and potential (b). U = 15 kV, for the needle-to-plane with d = 8.5 mm.

Even at a relatively low voltage at a tip with a small radius of curvature, the electric field reaches 10^6 V/cm. This field in the presence of microprotrusions [11] on the cathode, as well as nanoparticles [12], is sufficient for the emission of the first electrons from the cathode. Due to the high electric field, part of the emitted electrons, as well as part of the electrons that appeared due to gas ionization, go into the runaway mode and SAEB current is measured behind the anode with the collector. It should be noted that the value of the potential decreases with distance from the tip more slowly than the electric field. Accordingly, electrons without the participation of the streamer front [13] can gain only energy eU^* (e – charge of electron, U^* – potential in this point of gap). Upon initiation of SAEB, as was established in our works [8–10], a streamer forms near the tip due to REs. Figs.3–4 show the conditions under which the front of the streamer reached the anode; this led to the appearance of a step on the decay of the voltage pulse. Then, a diffuse discharge is formed in the gap, at which a further decrease in the voltage pulse amplitude is observed. In Fig.2, the magnitude of this step is small and it is hardly noticeable. However, a second step is visible in the voltage pulses, which is caused by the formation of a diffuse discharge. Note that SAEB behind the anode foil can be registered not only when the streamer reaches the anode and forms a diffuse discharge [8], but also during a corona discharge [14].

5. Conclusion

Studies have shown that SAEB generation is observed in a wide range of experimental conditions. At a generator voltage of tens of kilovolts and a voltage pulse rise time of 0.7, 4, and 200 ns, SAEB was recorded at air and nitrogen pressures of 25–100 kPa. It has been found that to register electron beams at low voltages, mesh anodes with a small cell size should be used. Such grids allow registering REs with relatively low energies, but significantly weaken the dynamic displacement current [10]. It follows from this work and the results of our previous studies [8–10] that the generation of REs initiates the formation of a streamer, the development of which leads to an initial drop in the voltage across the gap.

Acknowledgements

The reported study was performed within the framework of the State assignment of the IHCE SB RAS, project No. FWRM-2021-0014, as well as was funded by RFBR, project No. 20-02-00733.

6. References

[1] Wilson C.T.R., *Proc. Phys. Soc. London*, **37**, 32D, 1924; doi: 10.1088/1478-7814/37/1/314
[2] Tarasenko V.F., et al., *Plasma Devices and Operation*, **16**, 267, 2008; doi: 10.1080/10519990802478847
[3] Mesyats G.A., et al., *Trans. Plasma Sci*., **41**(10**)**, 2863, 2013; doi: 10.1109/TPS.2013.2258041
[4] Levko D., et al., J. *Appl. Phys.*, **111**, 013303, 2012; doi: 10.1063/1.3675527
[5] Shao T., Wang R., Zhang C., Yan P., *High Voltage*, **3**(1), 14, 2018; doi: 10.1049/hve.2016.0014
[6] Mesyats G.A., et al., *J. Appl. Phys.*, **116**, 063501, 2020; doi: 10.1063/1.5143486
[7] Tarasenko V., *Plasma Sources Science and Technol.*, **29**, 034001, 2020; doi 10.1088/1361-6595/ab5c57
[8] Beloplotov D.V., Tarasenko V.F., *J. Phys.: Conf. Series*, **1393**, 012004, 2019; doi 10.1088/1742-6596/1393/1/012004
[9] Beloplotov D.V., Sorokin D.A., Lomaev M.I., Tarasenko V.F., *Russ. Phys. Journal*, **62**, 1967, 2020; doi 10.1007/s11182-020-01930-x
[10] Beloplotov D.V., Tarasenko V.F., Shklyaev V.A., Sorokin D.A., *JETP Letters*, **113**(2) 129, 2021; doi 10.1134/S0021364021020053
[11] Mesyats G.A., *IEEE Trans. Plasma Sci.*, **23**, 879, 1995; doi 10.1109/27.476469
[12] Kalered E., et al., *Phys. Plasmas*, **24**, 013702, 2017; doi 10.1063/1.4973443
[13] Askar'yan G.A., *JETP Lett.*, **1**, 97, 1965;
[14] Kozyrev A.V., et al., *Atmosph. and Oceanic Optics*, **25**(2), 176, 2012; doi 10.1134/S102485601202008X